Heike Christopher (Autor)

A compact mode-locked diode laser system for high precision frequency comparison experiments

Leibniz Ferdinand Braun Institut

64

Innovationen mit Mikrowellen & Licht

Forschungsberichte aus dem Ferdinand-Braun-Institut, Leibniz-Institut für Höchstfrequenztechnik

A compact mode-locked diode laser system for high precision frequency comparison experiments

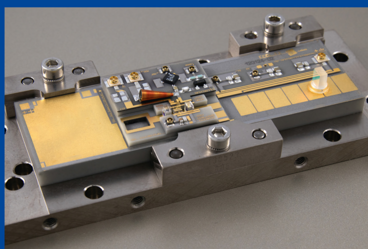

Heike Christopher

https://cuvillier.de/de/shop/publications/8418

Copyright:
Cuvillier Verlag, Inhaberin Annette Jentzsch-Cuvillier, Nonnenstieg 8, 37075 Göttingen, Germany
Telefon: +49 (0)551 54724-0, E-Mail: info@cuvillier.de, Website: https://cuvillier.de

1. Introduction

In the past two decades, optical frequency combs (OFCs) have become an invaluable tool in a multitude of applied science and fundamental physics applications. These range from, e.g., time keeping [1], to ranging [2], and sensing [3]. An emerging technology within the field of sensing are quantum optical sensors for, e.g., testing fundamental physics models [4–7]. The vast potential of OFCs was acknowledged in the awarding of the Nobel Prize in Physics to J. Hall and T. Hänsch in 2005 [8, 9].

Typical optical frequency comb generators (OFCGs) provide an optical spectrum spanning at least one octave or more [10]. This ultra-broadband optical spectrum allows for absolute stabilization of the OFC [11] providing the means to measure optical frequencies absolutely [12] and for comparing optical frequencies hundreds of THz apart [13]. The laser systems required to enable this are based on mode-locked solid-state [14] or fiber [4] lasers, or nonlinear processes in, e.g., micro-resonators [15]. Additionally, these highly complex laser systems typically comprise an optically pumped laser medium, high power pump diode lasers, elements for spectral broadening, beam shaping and distribution optics, as well as dispersion control elements. Though efforts are made to miniaturize the OFC generators, see, e.g., Refs. [4, 16], their complexity, power consumption, and footprint are still significant. Thus, the implementation of absolute stabilized OFCs in highly compact out-of-the-lab systems for field applications remains a formidable challenge.

Considerable reduction of OFC system complexity can be achieved for those applications that base on frequency comparison rather than absolute frequency determination [17]. Here, only control of the spectral distance between the individual comb lines is required and absolute stabilization of the OFC is not necessary. Further alleviation of system complexity is possible for those applications that compare frequencies spaced only few or tens of THz. The OFCs employed within such applications only need to cover the specific frequency interval between the frequencies of interest. This can allow for the omission of additional spectral broadening elements and can enable use of the OFC directly emitted from the mode-locked laser. However, the need for optical pumping still makes mode-locked solid-state or fiber lasers cumbersome devices. Additionally, control of the comb line spacing is not easily achieved for those lasers.

In contrast, mode-locked diode lasers offer not only control of their emission characteristics through electrical bias, diode lasers can also be integrated into miniaturized laser modules. These feature the level of compactness, robustness, and integrability that makes them ideal candidates for applications in the field and even in space [6, 18–20]. Moreover, compound semiconductors provide emission in most of the optical spectrum from the ultraviolet (UV) to the mid-infrared (IR) spectral range [21]. Since its first documentation in the 1970s, mode-locking of diode lasers has become a well established technology across the accessible spectral range [22–25]. For these lasers direct control of the comb line spacing is achieved via manipulation of the electrical bias [24].

One application that would greatly benefit from a diode laser-based OFC in the wavelength range around 780 nm are the QUANTUS (*Quantengase unter Schwerelosigkeit*; quantum gases under weightlessness) experiments. These aspire to implement a quantum test of the universality of free fall (UFF) in space by means of comparing the rate of free fall of different atomic species, rubidium (Rb) and potassium (K) [6, 26–31]. Employing the respective D2 transitions, an OFC spanning about 13 nm (approx. 7 THz) from 767 nm (approx. 391 THz) to 780 nm (approx. 384 THz) is required to facilitate frequency comparison and control experiments.

A similar spectral bandwidth of about 9 THz has already been reported for mode-locked diode lasers in the wavelength range around 830 nm [32]. Further, a diode laser-based OFC has been reported to be used as a means to control very closely spaced optical frequencies around the D2 transition of Rb [33]. Another, more recent diode laser-based approach utilized to generate an OFC is to inject the emission of a diode laser into a whispering gallery mode (WGM) microresonator [34–36]. When the diode laser's emission frequency is appropriately detuned relative to the resonance frequencies of the WGM microresonator, an OFC is generated that can span more than one octave. These OFCs are typically centered in the wavelength range of 1550 nm. However, some of those OFC even extend down to around 780 nm when the diode laser's power is strongly amplified by a fiber amplifier before injection into the WGM microresonator [34]. However, at the beginning of this work, to the best of my knowledge, no diode laser-based OFCs existed in the wavelength range around 780 nm that provided the spectral bandwidth required for the QUANTUS experiments, and no diode laser-based OFCG[1] was available that provided the compactness and robustness required for experiments carried out at a drop tower or in space.

The scope of this thesis, thus, is the development of a diode laser-based OFC which provides a spectral bandwidth of more than 13 nm in the wavelength range around 780 nm for use in future spaceborne QUANTUS experiments.

To introduce this thesis' scope in more detail, the OFC as a tool for determination and control of optical frequency differences is first discussed in the subsequent section. Then, the idea of the QUANTUS experiments is presented and an advanced frequency stabilization scheme for future QUANTUS experiments is sketched. Further, the status of the laser technology development for the QUANTUS experiments at the beginning of this thesis work is described. Requirements on a diode laser-based OFC for future QUANTUS experiments are identified. An overview of the state of the art of OFCs in the wavelength range around 780 nm is given. This chapter closes by highlighting the goals and outline of this thesis.

1.1. The optical frequency comb

Soon after the dawn of the laser [38, 39], generation of ultra-short (optical) pulses has been observed, see e.g. Refs. [40–46]. Shortly afterwards in the early sixties, phase locking of the longitudinal modes of a laser, also called mode-locking, was identified to be the underlying mechanism producing those ultra-short pulses [47–50]. A prerequisite for successful mode-locking

[1] Parallel to the beginning of this thesis work, first tests of a drop-tower suitable fiber-based OFCG were carried out [37]. However, this OFCG occupied the whole catapult capsule and was, thus, by far not compact enough for implementation within the QUANTUS experiments.

is an equidistant frequency separation between the longitudinal modes making up the optical spectrum of the laser [51, 52]. That comb-like optical spectrum produced by an ultra-short pulse mode-locked laser, see schematic in Fig. 1.1, is known as an OFC.

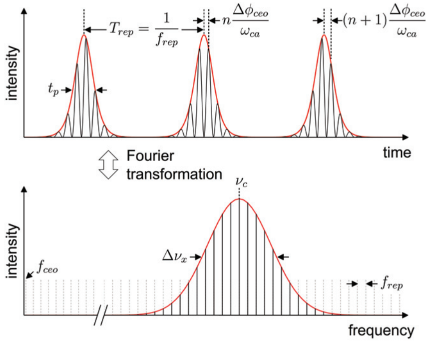

Figure 1.1.: Schematic of an optical frequency comb (solid black lines in bottom graph). In the time domain (top) the OFC is determined by a train of n pulses featuring a composition of a carrier frequency ω_{ca} (black) and an envelope function (red) with a width of t_p, a periodicity T_{rep}, and a carrier-envelope-offset (carrier-envelope-offset (CEO)) phase slip $\Delta\phi_{ceo}$. In the optical frequency domain (bottom) the OFC is determined by an envelope function (red line) with a center frequency ν_c, an inter-mode spacing equal to the pulse repetition rate f_{rep}, a spectral bandwidth $\Delta\nu_x$ at x dBc, and a CEO frequency f_{ceo}.

Measurement of optical frequency differences by means of an OFC generated by a mode-locked laser was first conducted in the late seventies [17]. Then, only a frequency interval of 1 GHz was bridged. Twenty years later, the frequency comb technique matured to allow for measurements of frequency intervals of tens of THz, and also of absolute frequencies [12, 53, 54]. Absolute frequency measurement can be facilitated by means of stabilizing the pulse repetition rate of the OFC, and stabilizing one of its comb lines to an atomic reference. The development of OFCs spanning more than one octave [55, 56] then provided the means for phase-coherent measurements of optical frequencies [57]. Since the first demonstration of an absolute stabilized OFC spanning more than one octave, employment of such an OFC as an optical ruler for precise measurements of absolute optical frequencies and frequency differences has become well-established [58–62].

For the future QUANTUS experiments in which the OFC developed within this thesis is to be employed, however, phase-coherent frequency measurement and comparison is not required. For these experiments, an OFC suitably spanning the wavelength range of interest (approx. 13 nm, and covering the K and Rb D2 transitions), and featuring suitable spectral and mechanical characteristics is envisioned.

In the following, the tool OFC is presented. To that end, a theoretical description of an OFC and a phenomenological description of its build-up is discussed. Further, measurement of optical frequencies and frequency differences by means of an OFC is introduced.

1.1.1. Theoretical description of mode-locked operation

The subsequent description follows Ref. [63].

The time-dependent electrical field of a single optical pulse is a composition of a carrier of frequency ω_{ca} and an envelope function $\hat{E}(t)$ written in complex notation as

$$E_p(t) = \hat{E}(t) \cdot \exp\left[\, i \cdot (\omega_{ca} t + \phi_{ceo})\right] \tag{1.1}$$

where ϕ_{ceo} is the carrier-envelope-offset (CEO) phase. For a pulse train consisting of identical pulses with a periodicity T_{rep} traveling through a non-dispersive medium, so that ϕ_{ceo} can be considered constant, the electrical field is given as

$$E(t) = \sum_n E_p(t - nT_{rep}). \tag{1.2}$$

In case of a pulse train traveling through a dispersive medium, however, the CEO phase evolves from pulse to pulse by an amount $\Delta\phi_{ceo}$ due to the difference in phase and group velocity. Thus, the n-th pulse experiences $\phi_{ceo,n} = n\Delta\phi_{ceo} + \phi_0$, where ϕ_0 is the CEO phase at time zero, see schematic in Fig. 1.1. The electric field of the pulse train is then given in the time domain as

$$E(t) = \sum_n \hat{E}(t - nT_{rep}) \cdot \exp\left[\, i\left(\omega_{ca} t + n(\Delta\phi_{ceo} - \omega_{ca} T_{rep}) + \phi_0\right)\right]. \tag{1.3}$$

This corresponds to

$$E(\omega) = \mathrm{e}^{i\phi_0} \mathfrak{F}(\hat{E})(\omega - \omega_{ca}) \sum_m \delta(\Delta\phi_{ceo} - \omega T_{rep} - 2\pi m) \tag{1.4}$$

in the frequency domain where $\mathfrak{F}(\hat{E})(\omega)$ is the Fourier-transform of $\hat{E}(t)$.

If ϕ_0 is equal for all pulses, as assumed in Eq. 1.3, the optical spectrum of the mode-locked pulse train consists of equally spaced spectral lines of frequency

$$\nu_m = m f_{rep} + f_{ceo} \tag{1.5}$$

where

$$f_{ceo} = \Delta\phi_{ceo} f_{rep}/(2\pi) \tag{1.6}$$

is the CEO frequency and

$$f_{rep} = \frac{1}{T_{rep}} = \frac{c_0}{2 n_g L_{res}}, \tag{1.7}$$

is the pulse repetition rate. The pulse repetition rate is given by the inverse of the round trip time T_{rep} (periodicity) of the pulses in the laser resonator. It is calculated using the vacuum speed of light c_0, the group refractive index n_g, and the length of the laser resonator L_{res}. The identity of the inter-mode spacing in the frequency domain and the pulse repetition rate in the time domain has been verified experimentally [53].

The laser intensity $I(t) \propto |E(t)|^2$ features the same periodicity as well. Using the intensity distribution in the optical frequency domain, typical characteristics of the frequency comb such as center frequency (center of gravity) ν_c and the spectral bandwidth $\Delta\nu_x$ at x dBc are determined, see Fig. 1.1. Including the time domain, characteristics such as the pulse width t_p, typically determined at full width at half maximum (FWHM) intensity, can be quantified, see Fig. 1.1.

1.1.2. Phenomenological description of mode-locked operation

Build-up of an OFC can phenomenologically be described as follows.

A free-running laser without any frequency-selective element features a multitude of longitudinal optical modes with random phases. This case is illustrated in Fig. 1.2(left). Mode competition leads to large fluctuations in the instantaneous frequency and the emitted intensity, see Fig. 1.2(bottom left).

Spontaneous locking of (some) modes occurs when the modes have a constant (locked) phase relationship [64, 65]. A spontaneously mode-locked wave packet forms. Maintaining the constant phase relationship between the spontaneously locked modes allows this spontaneously formed wave packet to travel back and forth in the laser resonator. In this case, a mode-locked optical pulse is emitted from the laser at time intervals T_{rep} corresponding to the resonator length, see Fig. 1.2(right). Further modes can lock to the wave packet during its travel in the laser resonator. This results in an increase of peak intensity of the wave packet compared to the case of only spontaneously locked modes, see Fig. 1.2(bottom).

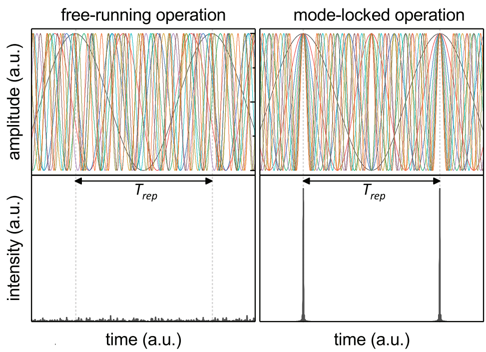

Figure 1.2.: Schematic of the temporal distribution of multiple emitted longitudinal modes at a fixed point outside the laser resonator: individual electric fields of (top, 10 modes for better visibility of the individual modes) and their intensity (bottom, 100 modes for better comparison of free-running and mode-locked operation) in a free-running (left) and (right) mode-locked laser. Free-running operation features random phases between the modes where spontaneous locking of some modes can occur. In mode-locked operation, in contrast, a phase-locked relationship between the modes exists and leads to build-up of a wave packet in the laser resonator.

The wave packet can be maintained in the laser resonator if it experiences more optical net-gain than the non-phase locked modes. This can be facilitated either by an element internal or external to the laser resonator.

An external element is realized by, e.g., modulating the optical gain or losses of the laser at a frequency corresponding to the inverse of the round trip time T_{rep} of the wave packet in the laser resonator. Here, a signal generator providing the modulation signal is required.

In contrast, an internal element is realized by, e.g., inserting a nonlinear element into the laser resonator that provides less optical losses for higher optical powers. Thus, the power-dependency of that internal element results in an overall net-gain for the appropriately mode-locked wave packet and net-loss for the other, still free-running optical modes of the laser resonator. Such an element is called a saturable absorber. Depending on the position of the saturable absorber in the laser resonator, the wave packet is emitted from the laser resonator with a rate that corresponds to the inverse round trip time or its harmonics [24, 66, 67]. In the former case, a single wave packet travels inside the laser resonator. This is called fundamental mode-locking. In the latter case, multiple wave packets are generated in the laser resonator. This case is called harmonic mode-locking.

1.1.3. Measurement of optical frequencies and frequency differences

Determination of an unknown optical frequency ν_1 (Fig. 1.3) by means of an OFC can be realized in a two-step measurement, see, e.g., Ref. [68]. In the first step, the comb line number m_{c1} of the closest comb line ν_{c1}, see Eq. 1.5, is ascertained using, e.g., a wavelength meter that provides sufficient measurement resolution ($\Delta\nu_{res} \ll f_{rep}/2$). In the second step, a beat note measurement between this OFC and the unknown optical frequency is performed yielding a microwave (radio frequency (RF)) frequency $|f_{b1}| = |\nu_1 - \nu_{c1}|$ that can precisely be detected by a frequency counter. Assuming $\nu_{c1} < \nu_1$ as shown in Fig. 1.3, the optical frequency under investigation is then given as

$$\nu_1 = \nu_{c1} + f_{b1} = m_{c1} f_{rep} + f_{ceo} + f_{b1}. \tag{1.8}$$

The sign of f_{b1} can be determined from the frequency position of ν_1 relative to ν_{c1} in the first step by, e.g. controlled breathing of f_{rep}. A consequence of Eq. 1.8 is that absolute control of all parameters of the OFC, i.e. the pulse repetition rate f_{rep} and the CEO frequency f_{ceo} is essential for accurate determination of an unknown optical frequency.

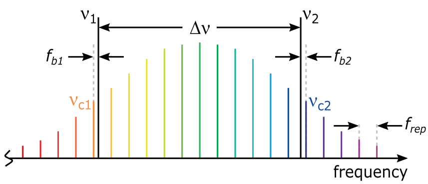

Figure 1.3.: Measurement of optical frequencies and frequency differences.

Frequency differences between two lasers can be determined in a similar way, yielding

$$\Delta\nu = \nu_1 - \nu_2 = (m_{c1} - m_{c2})f_{rep} + (f_{b1} + f_{b2}) \tag{1.9}$$

which only requires

(i) determination of the two comb line numbers m_{c1} and m_{c2},

(ii) determination of the repetition rate f_{rep}, and

(iii) counting of the RF beat note (in this case the sum frequency) between the two optical beat notes f_{b1} and f_{b2} derived from overlapping the two lasers with the OFC.

Thus, in contrast to absolute optical frequency measurements, comparison of two optical frequencies by measurement of their frequency difference eliminates the need to analyze and control the CEO frequency f_{ceo}, see Eq. 1.9. Further, if only variations in the frequency difference are of interest, then observing a microwave beat note of the two optically generated beat notes f_{b1} and f_{b2} is sufficient. While knowledge of the number of comb lines between the two frequencies under investigation is not necessary here, stabilization of the pulse repetition rate f_{rep} is essential to not produce frequency noise induced variations in the final beat note. An additional measurement of the pulse repetition rate, however, allows for determination of its (residual) frequency fluctuations which can then be observed in the determination of the frequency difference of interest.

Thus, the implementation of an OFC spanning only the spectral bandwidth of interest for measurement of frequency differences is possible. With this, the complexity of the required laser system can be minimized.

1.2. A tailored optical frequency comb for a spaceborne experiment

The development of a tailored OFC, which was conducted within this thesis work, was motivated by an application in the field of inertial sensing: a quantum sensor for testing the weak equivalence principle (WEP), also known as the universality of free fall (UFF). Such tests are of interest since quantum theories predict violations of the WEP [27, 69]. These violations could, to date, neither be confirmed nor rejected by experiment. For quantum sensor-based tests, the accuracy has been limited by, e.g., a too large thermally induced spread of the test masses, limited interrogations times, and residual accelerations in the experimental chamber [27]. One experimental series intending to push the accuracy for tests of the UFF are the QUANTUS (*Quantengase unter Schwerelosigkeit*; quantum gases under weightlessness) projects, see, e.g., Refs. [6, 28, 30, 31, 70].

The framework of the QUANTUS collaboration encompasses not only the test of the UFF itself, but also the development of the technology required to successfully conduct the experiments on micro-gravity platforms, first in the drop tower of the ZARM (*Zentrum für angewandte Raumfahrttechnologie und Mikrogravitation*; Center of Applied Space Technology and Microgravity) and later also onboard of sounding rockets. The development of the laser technology was facilitated within the LASUS (*Entwicklung von neuartigen Diodenlasersystemen für Präzisionsexperimente unter Schwerelosigkeit für zukünftige TEXUS-Missionen*; Development of novel diode laser systems for precision experiments under weightlessness for future TEXUS missions) project series. This thesis work was also conducted within the framework of the LASUS projects for the QUANTUS experiments.

In this section, the objective of the QUANTUS experiments is introduced. An advanced frequency stabilization scheme for future QUANTUS experiments is presented. Here, the advantage of employing an OFC is highlighted. Then, the status of the diode laser technology that had been developed within LASUS specifically for the QUANTUS experiments until the beginning of this thesis work is described. This section closes with identifying the requirements on a diode laser-based OFC for spaceborne tests of the UFF in the QUANTUS experiments.

1.2.1. The QUANTUS experiments: a test of the universality of free fall

The QUANTUS collaboration has made it its objective to employ the enhanced sensitivity of quantum sensor technology, particularly of light pulse atom interferometry, in microgravity to push the limit of measurement sensitivity for gravitational acceleration [70]. A light pulse atom interferometer is an inertially sensitive Mach-Zehnder-type matter wave interferometer in which the wave character of matter (atoms) is exploited to measure the inertial acceleration caused by the gravitational force of the earth [71]. Manipulation of the atoms (beam splitting, redirection, and re-combining) and read-out of the atom interferometer is facilitated by well-defined light pulses from high power, narrow linewidth continuous wave (CW) diode lasers.

With a suitably oriented apparatus, the accumulated interferometer phase shift due to gravitational acceleration is given by

$$\Phi = k_{eff} a T^2, \tag{1.10}$$

with the effective wave vector of the counter-propagating light pulses of the atom interferometer

$$k_{eff} = |\vec{k}_1 - \vec{k}_2| \approx 2k = 4\pi/\lambda = 4\pi\nu/c_0 \tag{1.11}$$

with wavelength λ (frequency ν, vacuum speed of light c_0), the local acceleration a and the interrogation time T between the light pulses [27]. The relative amount of atoms in the two output states of the interferometer allows for determination of Φ.

It can be seen in Eq. 1.10 that the sensitivity for measuring a scales quadratically with the interrogation time T. Hence, large interrogation times are advantageous. One of the major benefits of conducting experiments in a micro-gravity environment is the accessibility of these large interrogation times due to the lack of gravitational pull on the test masses (the atoms) towards the experimental chamber's wall. Additionally, weightlessness offers benefits such as improved preparation of the test masses [31, 70]. Further, in a micro-gravity environment vibrational (acceleration) noise due to, e.g., seismic activity of the earth can be minimized or even eliminated.

A test of the UFF can be performed with a light pulse atom interferometer by comparing the gravitational acceleration a_1 and a_2 of two different atomic species in simultaneously conducted experiments. The difference in acceleration is expressed by the Eötvös ratio [27]

$$\eta = 2\frac{a_1 - a_2}{a_1 + a_2} \tag{1.12}$$

which is non-zero in case of the violation of the UFF. Using K and Rb atoms as test masses in the same experiment simultaneously, as planned in future QUANTUS experiments [27], offers several advantages [27, 30, 70, 72, 73]. First, the cooling mechanisms and the interactions of Rb and K vapor mixtures are well-known [27]. Both atomic species feature a large difference in mass, and a large variety of isotopes. Second, similar wavelengths of respective D2 transitions of K and Rb, approx. 767 nm and 780 nm, respectively, allow for simplification of the laser system design by use of the same optics, e.g., mirrors and retardation plates, as well as shared optical fibers and a shared interferometry setup. Further, diode laser technology can be applied as frequency comparison with an OFC requires only modest optical bandwidth (BW) of the OFC.

Systematical errors, however, limit the measurement accuracy. A differential measurement approach minimizes some noise sources by common mode rejection. Nevertheless, precise control of the optical frequencies (via $k_{eff,i} \approx 2k_i$ of each atomic species) is a fundamental requirement for the experiment's success. In existing setups of the QUANTUS collaboration, individual frequency stabilization of two lasers emitting at around 767 nm and 780 nm to a K and Rb atomic reference, respectively, is performed. Hence, the determination of the respective k_{eff} is limited by the accuracy of the respective spectroscopy-based frequency stabilization. Further, knowledge of the frequency difference between the K and the Rb interrogation lasers is also limited by the spectroscopy-based frequency stabilization. However, referencing both lasers to a common atomic reference (e.g. Rb) would allow to omit the other atomic reference (e.g. K) and the associated uncertainty. A stabilization scheme implemented with an OFC that can bridge the required frequency region spanning the approx. 13 nm (6.8 THz) from the Rb to the K D2 transition frequency, about 384.23 THz ($\approx$ 780.24 nm) and 391.02 THz ($\approx$ 766.70 nm), respectively, would be of advantage for successful implementation of future experiments.

1.2.2. An advanced frequency stabilization scheme for future QUANTUS experiments

In essence, an advanced stabilization scheme can be understood as a determination of the frequency difference of the K and Rb interrogation lasers, see Fig. 1.4(a). This scheme can be facilitated by an OFC of which the pulse repetition rate has been stabilized to a microwave reference f_{ref}. A schematic for a potential frequency control in future QUANTUS experiments is sketched in Fig. 1.4(b). The electronics are shown in blue and the optical components are sketched in black. The reference signals (f_1, f_2, f_{ref}) feature a common frequency reference.

Firstly, the pulse repetition rate of the OFC is stabilized to a reference providing a reference frequency of, e.g., $f_{ref} = 6.8$ GHz. This allows for use of similar electronics as for the preparation of the interferometry beams, simplifying the electronics system. The optical frequency of the reference laser for the Rb experimental part (CW 780 nm) is frequency-stabilized by means of a Rb vapor cell. Then, one comb line of the OFC is frequency-stabilized to the Rb reference laser. To precisely control the CEO frequency of the OFC, the phase of the RF beat note signal between the Rb reference laser and the above-mentioned comb line of the OFC is compared to the frequency of a RF frequency reference with an appropriately selected frequency f_1, and the resulting phase error is fed back to the CEO frequency of the OFC.

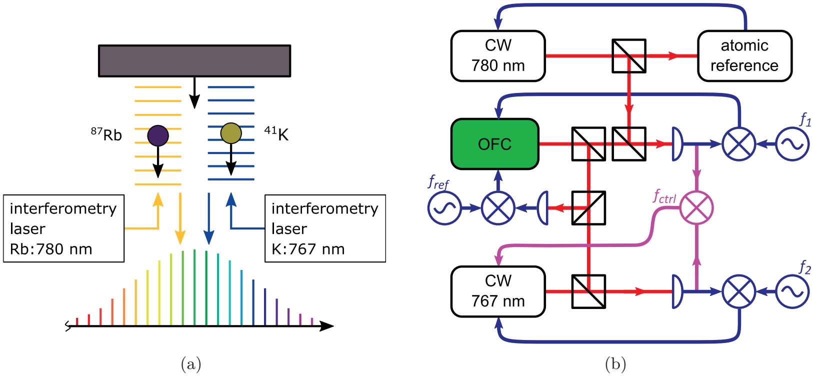

Figure 1.4.: Schematic of an advanced (a) frequency comparison and (b) frequency control for future QUANTUS experiments. The reference signals (f_1, f_2, f_{ref}) feature a common frequency reference.

Secondly, frequency comparison of the reference lasers for K and Rb is conducted with the OFC in order to offset stabilize the reference laser of the K part relative to that of the Rb part. To this end, the optical frequency of the K reference laser (CW 767 nm) is compared to that of the closest comb line of the OFC. A control signal for the K reference laser is then generated by comparison of the phase of the RF beat note signal between the OFC and the K reference laser and a second RF frequency reference f_2, the frequency of which is set appropriately. Alternatively, the beat note signals of the reference lasers for the K and Rb experiment parts and the respective closest comb lines of the OFC can be directly compared to generate a control signal f_{ctrl} for the K reference laser (sketched in pink). In this alternative scenario, a stabilization of the OFC to the Rb atomic reference, which would imply an absolute stabilization of the OFC, is not necessary, see Eq. 1.9.

The stabilization scheme, however, depends directly on the RF linewidth Δf_{rep} of the pulse repetition rate as can be illustrated as follows. Employing the stabilization scheme sketched in pink in Fig. 1.4(b), the frequency stability of the Rb laser is transferred to the K reference laser via the OFC. Thus, the K frequency ν_K can be described by

$$\nu_K = \nu_{Rb} + \Delta\nu = \nu_{Rb} + \nu_{trans} + f_{b-Rb} + f_{b-K} \tag{1.13}$$

where ν_{Rb} is the Rb laser's frequency, and f_{b-Rb} and f_{b-K} are the RF beat note frequencies of the comb lines closest to the Rb and K D2 transition frequencies with the K and Rb lasers, respectively. The frequency ν_{trans} is the part of the frequency difference between the frequencies of the K and Rb lasers that is directly bridged by the OFC.